



# MODIFIED CHEMICAL REACTION IN THE MHD WILLIAMSON FLOW NICKEL CHROMIUM IRON ALLOY (NIMONIC 80A) -KEROSENE NANOFLUID OVER A THIN NEEDLE

<sup>1</sup>Tapas Datta,

Department of Mathematics, A.K.P.C. Mahavidyalaya, Subhasnagar, Bengai, Hooghly, West Bengal,  
India.

Ph.D scholar, Dr. A P J Abdul Kalam University, Indore, Madhya Pradesh - 452016

Email: tapasdatta9999@gmail.com

<sup>2</sup>Dr. Annapurna Ramakrishna Sinde,

Department of Mathematics, Dr. A P J Abdul Kalam University, Indore, Madhya Pradesh - 452016

E-mail: jayabhandari15@gmail.com

<sup>3</sup>Dr. Md Tausif Sk,

Department of Mathematics, Acharya B N Seal College, Cooch Behar – 736101, West Bengal, India

Email: tausifdropbox@gmail.com

1420

## Abstract:

The article outlined synthetically responding liquid stream with nanoparticles in it over a slender needle under a remotely applied attractive power field. The liquid of the stream viewed as non-Newtonian Williamson liquid. While building the stream model Brownian movement and thermophoretic peculiarities are thought about. Then, at that point, utilizing reasonable dimensionless changes the overseeing non straight halfway differential conditions are formed into non direct customary differential conditions alongside the limit conditions. Since the stream conditions couldn't be addressed logically, we apply mathematical shooting procedure and utilized MATHEMATICA programming to tackle it. The discoveries are then organized by means of different diagrams. The impacts of both homogeneous and heterogeneous compound response are seen in the article. It is investigated that presence of homogeneous substance response impact the temperature and nanoparticle thickness of the stream more actually than heterogeneous compound response. Additionally, Williamson Nimonic 80a-Kerosene Nanofluid show greater aversion to the synthetic response in the event of Nimonic 80a-Kerosene Nanofluid thickness.

**Keywords:** Homogeneous Chemical Reaction, Heterogeneous Chemical Reaction, MHD, Williamson nanofluid, thin needle.

**DOI Number:** 10.48047/NQ.2022.20.21.NQ99149

**Neuroquantology 2022; 20(21):1420-1434**

## Introduction:

Axisymmetric limit layer stream and intensity move process has more significance due to its modern and mechanical cycles. One sort of

axisymmetric stream is meager needles. A criticizing object with illustrative unrest is meager needle calculation. The stream is Axisymmetric for this situation and the limit



layers are nearer to the measurement of the slendering chamber. Slendering needle with sporadic thickness acquired a lot of sensible significance now a days as it shows a moving change in the field of biomimetics including blood stream issues, disease treatment, metal turning, optimal design, little estimating gear fabricating and so forth. Lee [1] introduced a condition administering the movement of an incompressible liquid streaming pivotally over a slender paraboloid of unrest. He talked about the asymptotic ways of behaving and a surmised arrangement, and registered the mathematical arrangements. He reasoned that for logically dainty needles, the relocation thickness and drag per unit length reduced gradually, yet ultimately become zero as the needle evaporated. Chen and Smith [2] researched constrained consistent laminar incompressible stream over dainty needles logically. They acquired temperature profile and nature of intensity move under the minor departure from nuclear energy regulation in wall temperature and surface intensity transition. They likewise analyzed the impact of needle size and Prandtl number on the warm profile of the stream. Ishak et al. [3] research the limit layer stream on a moving isothermal slight needle lined up with a moving stream. They tackled overseeing conditions mathematically by a limited contrast strategy. Double arrangements were found to exist when the needle and the free stream move in the contrary bearings. Ahmed et al. [4] changed limit layer conditions of consistent laminar blended convection limit layer stream of an incompressible gooey liquid along vertical dainty needles for both helping and contradicting stream and addressed mathematically utilizing a certain limited distinction conspire known as the Keller-box strategy. They had been found that the stream and intensity move qualities were fundamentally impacted by different boundaries like the blended convection boundary, the boundary an addressing the needle size, and Prandtl number. Trimbitas et al. [5] found that the strong volume portion influences the liquid stream and intensity move qualities. They likewise inferred that the arrangements exist up to a basic worth of  $\lambda$ ,

past which the limit layer isolates from the surface and the arrangement in light of the limit layer approximations is beyond the realm of possibilities. Then Sulochana et al. [6] concentrated because of thermophoresis and Brownian movement on 2D constrained convection of MHD Al50Cu50/H<sub>2</sub>O and Cu/H<sub>2</sub>O nanofluid stream. They saw that thermophoresis and Brownian movement improved warm conductivity of nanofluid at an extraordinary degree. Krishna et al. [7] legitimized that raising the needle size didn't affect the Blasius stream over moving even needle. The intensity move rate in the Sakiadis stream was high contrasted and that in the Blasius stream. Likewise, the intensity move rate in the Sakiadis stream was high contrasted and that in the Blasius stream. Sulochana et al. [8] worked out that rising the needle size fundamentally decreases the stream and warm fields of both nanofluids. Specifically, warm and speed fields of Fe<sub>3</sub>O<sub>4</sub>-methanol nanofluid are exceptionally devalued when compared with the Fe<sub>3</sub>O<sub>4</sub>-water nanofluid. The nanofluid stream which happens over a meager needle moving pivotally with uniform speed in the very bearing as that of the outside free stream is concentrated by Ahmed et al. [9]. Salleh et al. [10] inspected blended convection ferrofluid and did steadiness investigation too.

Nanofluids lately are viewed as fundamental in designing applications; however, they likewise assume an expressive job in late modern turns of events. Indeed, in the advanced world, an Earth-wide temperature boost and natural contamination unavoidably make energy emergencies. In this manner, for constant turns of events, specialists and researchers are looking for new energy creations. In light of the new headway in nanotechnology, the communication of nanoparticles is viewed as more helpful to develop warm proficiency of base liquids. Nanoparticles are additionally utilized as coolants in gigantic mechanical and modern frameworks. This thought was exuded by Choi and Eastman [11] and entranced the consideration of agents lately. Buongiorno [12] admonished the two fundamental highlights specifically

thermophoresis and Brownian viewpoints for the development of warmth move related with nanoparticles.

Hydrodynamic flows with magnetic field and slip have received pivot attention of researchers owing to wide significant and varied applications in industrial along manufacturing processes. As a rule, no-slip limit condition displays mistaken reports, as in frameworks like MEMs you no-slip is at this point not material. Bhaskar Reddy et al. [13] concentrated on MHD slip stream impacts on nanoflow. The impacts of Magnetic field along with slip system were tested by Sreenivasulu et al. [14]. Tamoor [15] investigated the thermal analysis of hydromagnetic slip flow through a cylinder in the account of thermally stratified medium. MHD slip flow with radiation and variable fluid properties was studied by Parida et al. [16]. Nayak et al. [17] examined the influence of variable magnetic field on 3D flow with radiation. Slip effects on MHD radiative nanofluid flow was discussed by Nayak et al. [18]. Das et al. [19] presented the hydromagnetic slip flow of radiative nanofluid with ramped wall temperature. Abbas et al. [20] studied slip effect on curved stretching surface. Tausif et al. [21] investigated the magneto-slip effect on permeable stretching surface. Farooq et al. [22] discussed stagnation point flow with magnetic field effects.

Bhatti et al. [23] executed the Buongiorno model to analyze the thermo-dispersion examination in Williamson nanofluid deluged in the permeable surface. The particular qualities of non-Newtonian liquids have been as of late concentrated immeasurably by different examiners as a result of their fascinating applications in the time of synthetic and mechanical businesses. These liquids are multidisciplinary and liked over reliably gooey liquids because of their incomparable rheological properties. Makeup, blood, black-top, stick, natural solvents, nectar prompts such class of liquids. Non-Newtonian liquids, because of their significant impacts, has various applications in the atomic fuel slurries, ointments, bio-liquids in organic tissue, polymeric fluid expulsion, emulsions and polymers, and some more.

Confused to the thick liquids, the rheology of non-Newtonian liquids can't be estimated by a solitary numerical articulation. In this manner, to feature such complex properties as viscoelasticity, shear thickening, diminishing and thixotropy, and so forth, some unconventional liquid models have been propounded in the writing. Amid such models, Williamson liquid is of them which fulfilled the shear diminishing (consistency declined with shear rate) properties. Naseer et al. [24] examined the progression of Williamson liquid over a vertically moving extending chamber. Hamid et al. [25] presented the mathematical recreations on the wedge stream of Williamson liquid within the sight of warmth move. They worried that the wedge point boundary successfully adjusted the thickness of the limit layer. The extending stream of Williamson liquid bookkeeping, the electric and magnetic field impacts, have been summed up by Hayat et al. [26]. The impedance of speed and warm slip in Williamson liquid stream screamed by a moving plate has been indicated by Lund and collaborators [27]. The 3D progression of Williamson-Casson liquid with heat assimilation/age and homogeneous-heterogeneous highlights were examined by Raju et al. [28].

Considering all the above articles in the literature, we proposed that the chemically reacting Williamson Nimonic 80a-Kerosene Nanofluid flow was flowing under the variable magnetic force field over thin needle. A modified model of chemical reaction both 1<sup>st</sup> order homogeneous and 3<sup>rd</sup> order heterogeneous chemical reaction is taken into consideration. To justify the presence of nanoparticle in the fluid, Brownian motion and thermophoresis effects are also considered to portray the flow model.

#### **Constitution of Mathematical model:**

A consistent laminar two-dimensional (2D) and an incompressible Axisymmetric limit layer transport of WilliamsonNimonic 80a-Kerosene Nanofluid through a flimsy needle is thought of. The flat thin needle with the sweep is  $r = h(x)$ , in which  $r$  and  $x$  speak to the spiral and hub facilitates individually the non-direct warm radiation impact is

considered in the energy condition. Here  $x$  is estimated from the needle driving and the edge should thin in which its thickness can't surpass that of the limit layer. A variable magnetic force field  $G = G(x) = G_0 x^{-0.5}$  is forced the other way to the flat slim needle, here  $G_0$  is the constant. Additionally, the initiated magnetic field is irrelevant attributable to the

magnetic Reynolds number and cross over applied magnetic field to be exceptionally little. It is viewed as that the needle moves evenly with the uniform speed  $U_{wall}$  in the two ways to the standard of the uniform speed  $U_\infty$ . The stream wonders along suspensions are shown in Fig.1.

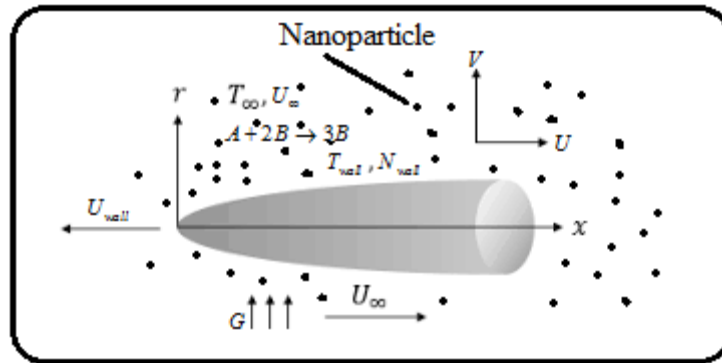


Figure 01: Physical model of the flow

The Mathematical model of Williamson liquid is characterized as [16]

$$S = \left\{ \mu_\infty - \left( \frac{\mu_\infty + \mu_0}{\Upsilon \Gamma - 1} \right) \right\} \Upsilon \quad (1)$$

Where  $\mu_\infty, \mu_0$  are the viscosity at infinity and zero shear rate,  $\Gamma$  the time constant and  $\Upsilon$  reads as

$$\Upsilon^2 = \frac{1}{2} \sum_i \sum_j \Upsilon_{ij} \Upsilon_{ji} = \frac{\Pi_s}{2} \quad (2)$$

Here  $\Pi_s$  the second invariant tensor.

The specialists favored this model as it might speak to the qualities of blood in the person. Here, the Nimonic 80a-Kerosene Nanofluid is used as the solution of chemical reactions. The autocatalyst 'A' flowstowards the flat sheet from the far field with a constant concentration  $A_\infty$ . In the boundarylayer region, the homogeneous reaction takes place, and is recognized as isothermal, cubic, and autocatalytic, i.e.  $A + 2B \rightarrow 3B$  Reaction rate =  $K_{HM} AB^2$ . There is no chemical reaction in the external flow so that the reaction rate at the outer edge of the

boundary-layer is zero. While on the catalyst surface, the heterogeneous reaction arises, which is single, isothermal, and of the first order, i.e.  $A \rightarrow B$  Reaction rate =  $K_{HT} A$ , here 'A' and 'B' are the concentrations of the species  $S_A$  and  $S_B$ , and  $K_{HM}$  and  $K_{HT}$  are the coefficients associated with the homogeneous and heterogeneous reactions, respectively. Based on the ideas of Buongiorno [12], the governing equations embodying the conservations of the total mass, the thermal energy, the chemical reactions, and the nanoparticle volume fractions are written by

$$\begin{aligned}
 \frac{\partial}{\partial x}(rU) + \frac{\partial}{\partial r}(rV) &= 0 \\
 U \frac{\partial U}{\partial x} + V \frac{\partial U}{\partial r} &= \frac{\nu_{nf}}{r} \left( 1 + \Gamma \sqrt{2} \frac{\partial U}{\partial r} \right) \frac{\partial}{\partial r} \left( r \frac{\partial U}{\partial r} \right) - \frac{\sigma G^2 U}{\rho} \\
 U \frac{\partial T}{\partial x} + V \frac{\partial T}{\partial r} &= \alpha_{nf} r^{-1} \frac{\partial}{\partial r} \left( r \frac{\partial T}{\partial r} \right) + \tau \left( D_{BM} \frac{\partial T}{\partial r} \frac{\partial B}{\partial r} + \frac{D_T}{T_\infty} \left( \frac{\partial T}{\partial r} \right)^2 \right) + \frac{\Delta H_{HR}}{(\rho c_p) \gamma_{SC}} K_{HM} AB^2 \\
 U \frac{\partial A}{\partial x} + V \frac{\partial A}{\partial r} &= D_A r^{-1} \frac{\partial}{\partial r} \left( r \frac{\partial A}{\partial r} \right) - K_{HM} AB^2 \\
 U \frac{\partial B}{\partial x} + V \frac{\partial B}{\partial r} &= D_B r^{-1} \frac{\partial}{\partial r} \left( r \frac{\partial B}{\partial r} \right) - K_{HM} AB^2 \\
 U \frac{\partial N}{\partial x} + V \frac{\partial N}{\partial r} &= D_{BM} r^{-1} \frac{\partial}{\partial r} \left( r \frac{\partial N}{\partial r} \right) + \frac{D_T}{T_\infty} r^{-1} \frac{\partial}{\partial r} \left( r \frac{\partial T}{\partial r} \right)
 \end{aligned} \tag{3}$$

The boundary condition of the flow is

$$U = U_{wall}, V = 0, -\kappa \frac{\partial T}{\partial r} = K_{HT} \frac{\Delta H_{HR}}{\gamma_{SC}} A, D_A \frac{\partial A}{\partial r} = -D_B \frac{\partial B}{\partial r} = K_{HT} A, N = N_{wall} \text{ at } r = h(x) \tag{4}$$

$U \rightarrow U_\infty, T \rightarrow T_\infty, A \rightarrow A_\infty, B \rightarrow 0, N \rightarrow N_\infty$  as  $r \rightarrow \infty$

Here (U,V) are velocity component in (x,r) direction,  $\Gamma$  material parameter,  $\nu$  dynamic viscosity,  $\rho$  density,  $\sigma$  electrical conductivity, T temperature,  $\alpha$  thermal diffusivity,  $\tau = (\rho c_p)_{np} / (\rho c_p)_f$  ration of specific heat capacity of nanoparticles and base fluid,  $D_{BM}$  Brownian Motion diffusion,  $D_T$  Thermophoresis diffusion,  $\Delta H_{HR}$  Heat reaction constant,  $\gamma_{SC}$  stoichiometric coefficient for the heterogeneous reaction,  $D_A$  and  $D_B$  are diffusion coefficient of  $S_A$  and  $S_B$  accordingly, N nanoparticle volume fraction,  $\kappa$  thermal conductivity.

$$\mu_{nf} = \frac{\mu_f}{(1 - \zeta)^{2.5}} \tag{5}$$

where  $\zeta$  is the solid volume fraction of nanoparticles. The effective density  $\rho_{nf}$ , thermal diffusivity  $\alpha_{nf}$  and the heat capacitance of the Nimonic 80a-Kerosene Nanofluid  $(\rho C_p)_{nf}$  are given by

$$\rho_{nf} = (1 - \zeta) \rho_f + \zeta \rho_s \tag{6}$$

$$\alpha_{nf} = \frac{k_{nf}}{(\rho C_p)_{nf}} \tag{7}$$

$$(\rho C_p)_{nf} = (1 - \zeta) (\rho C_p)_f + \zeta (\rho C_p)_s \tag{8}$$

**TABLE 1: THERMOPHYSICAL PROPERTIES OF REGULAR FLUID AND NANOPARTICLES:**

Physical Properties	Kerosene	Nimonic 80A
$C_p$ (J/ kg K)	2090	448
$\rho$ (kg/ m <sup>3</sup> )	780	8190
$\kappa$ (W/ mK)	0.149	112
$\alpha \times 10^7$ (m <sup>2</sup> / s)	1.47	116.3



$\beta \times 10^{-5} (1/K)$	99	8.8
------------------------------	----	-----

The thermal conductivity of Nimonic 80a-Kerosene Nanofluid restricted to spherical nanoparticles is approximated by the Maxwell [21]

$$\frac{\kappa_{nf}}{\kappa_f} = \frac{\kappa_s + 2\kappa_f - 2\zeta(\kappa_f - \kappa_s)}{\kappa_s + 2\kappa_f + 2\zeta(\kappa_f - \kappa_s)} \quad (9)$$

Here  $\mu_f$  is the consistency of the base liquid,  $\rho_f$  and  $\rho_s$  are the densities of the unadulterated liquid and nanoparticles, separately,  $(\rho C_p)_f$  and  $(\rho C_p)_s$  are the particular intensity boundaries of the base liquid and nanoparticles, individually,  $\kappa_f$  and  $\kappa_s$  are the warm conductivities of the base liquid and nanoparticles, individually.

As claimed, it is appropriate to assume that the diffusion coefficients of the chemical species A and B are of comparable sizes. This is useful for us to give the assumption that the diffusion coefficients  $D_A$  and  $D_B$  are equal. With this knowledge,  $A+B=A_\infty$ .

To solve the governing equations with boundary conditions we introduce the similarity transformation as below

$$\zeta = \frac{U_0 r^2}{\nu x}, \zeta = x f(\zeta), U = r^{-1} \frac{\partial \zeta}{\partial r}, V = -r^{-1} \frac{\partial \zeta}{\partial x}, \quad (10)$$

$$\vartheta(\zeta) = \frac{T - T_\infty}{T_{wall} - T_\infty}, A = A_\infty \phi(\zeta), \varphi(\zeta) = \frac{N - N_\infty}{N_{wall} - N_\infty}, h(x) = \left( \frac{\nu a x}{U_0} \right)^{0.5}$$

The converted governing equations are

$$2 \frac{\mu_{nf}}{\mu_f} (1 + We f'') (\zeta f'')' + \left( 1 - \phi + \phi \frac{\rho_{nf}}{\rho_f} \right) \left\{ ff'' - M (f')' \right\} = 0$$

$$\frac{\kappa_{nf}}{\kappa_f} (\zeta \vartheta')' + Pr \left\{ 1 - \phi + \phi \frac{(\rho c_p)_{nf}}{(\rho c_p)_f} \right\} \left\{ f \vartheta' + 2\zeta (N_B \vartheta' \varphi' + N_T (\vartheta')^2) + H_{HM} \phi (\phi - 1)^2 \right\} = 0 \quad (11)$$

$$Sc^{-1} (\zeta \phi'')' + \frac{1}{2} f \phi' - C_{HM} \phi (\phi - 1)^2 = 0$$

$$2(\zeta \varphi')' + Le f \varphi' + 2 \frac{N_T}{N_B} (\zeta \vartheta')' = 0$$

The boundary conditions are

$$f(a) = \frac{\lambda a}{2}, f'(a) = \frac{\lambda}{2}, \vartheta'(a) = -\kappa_{HM} \phi(a), \phi'(a) = C_{HT} \phi(a), \varphi(a) = 1 \quad (12)$$

$$f' \rightarrow \left( \frac{1 - \lambda}{2} \right), \vartheta \rightarrow 0, \phi \rightarrow 1, \varphi \rightarrow 0$$

where  $We$  is the Weissenberg number,  $M$  is magnetic factor,  $Pr$  is the Prandtl number,  $N_B$  is the Brownian motion parameter,  $N_T$  is the thermophoresis parameter,  $H_{HM}$  is the homogeneous reaction heat parameter,  $\kappa_{HM}$  is the thermal conductivity due to the homogeneous reaction,  $C_{HM}$  is the strength coefficient of the homogeneous reaction,  $Le$  is the Lewis number, and  $C_{HT}$  is the strength parameter due to the heterogeneous reaction,  $\lambda$  is velocity ratio parameter, which are defined by

$$We = \frac{\sqrt{2} \Gamma U_0^3}{\nu_f x}, M = \frac{\sigma G_0^2}{\rho_f U_0}, N_B = \frac{D_{BM} (N_{wall} - N_\infty)}{\nu}, H_{HM} = \frac{K_{HM} \Delta H_{HR} A_\infty^3}{\gamma_{SC} (\rho c_p)_f (T_{wall} - T_\infty)}, \lambda = \frac{U_{wall}}{U_\infty}, U_0 = U_{wall} + U_\infty \neq 0$$

$$C_{HM} = \frac{K_{HM} A_\infty^3}{U_0}, \kappa_{HM} = \frac{\nu K_{HT} A_\infty \Delta H_{HR}}{\kappa (T_{wall} - T_\infty) \gamma_{SC} U_0}, C_{HT} = \frac{K_{HT} U_0}{\nu D_A}, Le = \frac{\alpha}{D_{BM}}, N_T = \frac{D_T (T_{wall} - T_\infty)}{T_\infty \nu}, Sc = \frac{\nu}{D_B}, Pr = \frac{\nu}{\alpha}$$

To view the trends of heat and mass transference of the fluid system of the current

paper, authors have introduced terms like Nusselt number  $Nu$  which designates heat





transmission rate and Sherwood number  $Sh$  which presents mass transmission rate (wall species diffusion rate). Also, we have calculated that  $Nu \propto -\theta'(a)$  and  $Sh \propto -\phi'(a)$ . So we assume that local Nusselt number  $Nur = -\theta'(a)$  and local Sherwood number  $Shr = -\phi'(a)$ .

**Solution Scheme:**

The set of equations (11) with boundary conditions (12) is highly non-linear and coupled and therefore the system cannot be solved analytically. Therefore, they are solved in the symbolic computation software MATHEMATICA using shooting technique. It would be impractical to solve the system for even a very large finite interval. So, effort has been made to solve a sequence of problems posed on increasingly larger intervals to verify the solution's consistent behavior as the boundary approaches to 'a'. The plot of each

successive solution has been superimposed over those of previous solutions so that they can easily be compared for consistency. For numerical computation infinity condition has been taken at a large but finite value of  $\zeta$  where no considerable variation in temperature, concentration, etc. occurs.

**Validity of solutions:**

Using the above mentioned scheme we solved the 1<sup>st</sup> equations of (11) with the value of  $\lambda=0$ ,  $We=0$  and  $M=0$  and the boundary conditions are  $f(a)=0, f'(a)=0, f'(\infty)=\frac{1}{2}$  and obtained the values of  $f''(a)$  with various values of 'a'. Then compare our findings with the Chen and Smith [2] and Ishak et al. [3]. Here we observe our results have excellent degree of agreement with the already established work.

Table 1: Various values of  $f''(a)$  for various values of 'a'

'a'	Present research	Chen and Smith [2]	Ishak et al. [3]
0.1	1.288705	1.28881	1.288801
0.01	8.4923901	8.49244	8.492412
0.001	62.162048	62.16372	62.16371

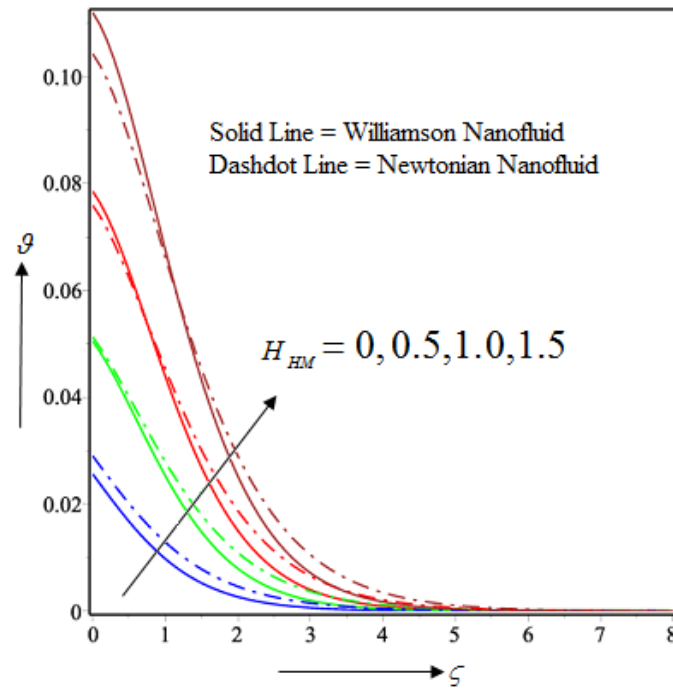
**Results and Discussions:**

Our aim is to constitute a flow model of Williamson Nimonic 80a-Kerosene Nanofluid flow over a thin needle with modified homogeneous and heterogeneous chemical reaction in it. We compare our results depicting the effects of chemical reaction on the heat and mass transfer of the flow between Newtonian and Williamson nanofluid.

**Temperature profile of the flow:**

The influence of  $H_{HM}$  on the temperature of the flow is observed in figure 2. It illustrated that increase in  $H_{HM}$  elevated the heat production in the flow due to homogeneous chemical reaction. Hence the temporal profile of the flow increases. Also, the temperature of the Newtonian fluid is less near the flow surface but after some distance from the needle surface the temperature of the Williamson fluid





1427

Figure 02:  $H_{HM}$  on the temperature of the flow

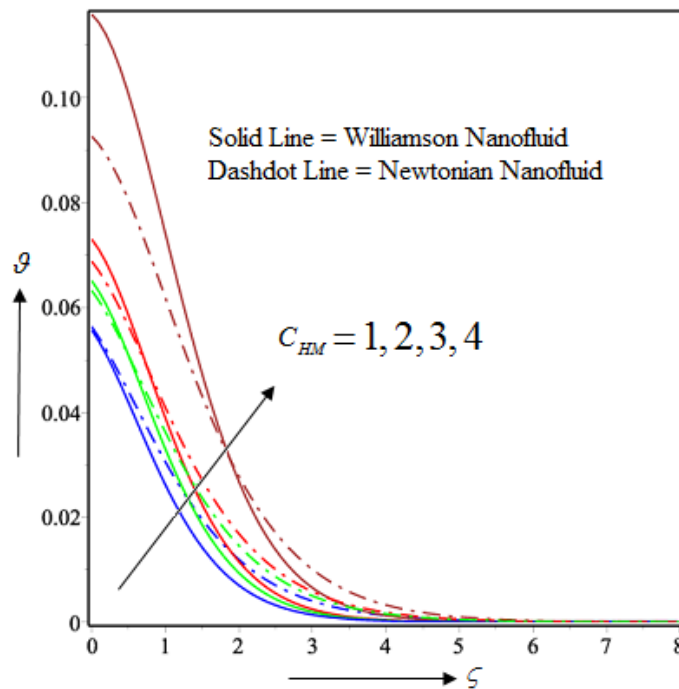


Figure 03:  $C_{HM}$  on the temperature of the flow

diminishes than Newtonian fluid. Similarly rise in  $C_{HM}$  increases the homogeneous chemical reaction in the flow. Therefore heat generation also increases of the flow (Figure 3). Here the deference of temporal



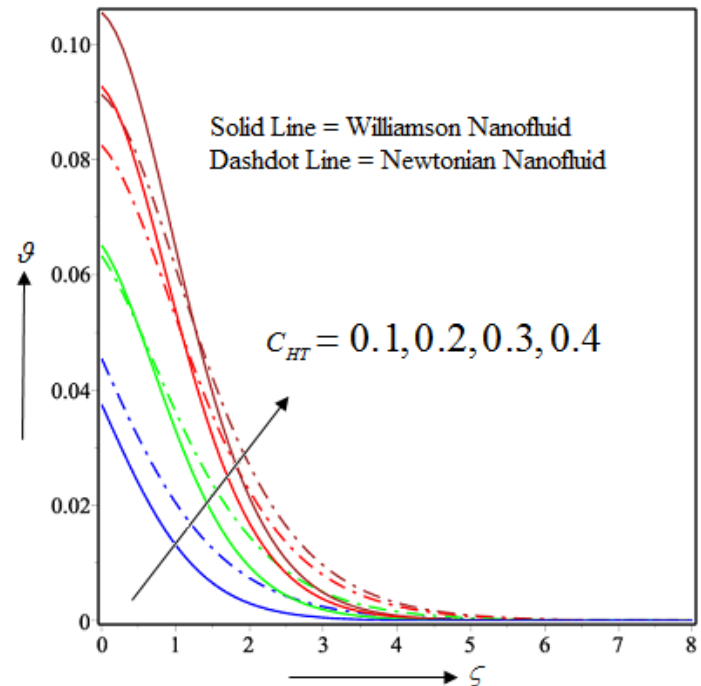


Figure 04:  $C_{HT}$  on the temperature of the flow

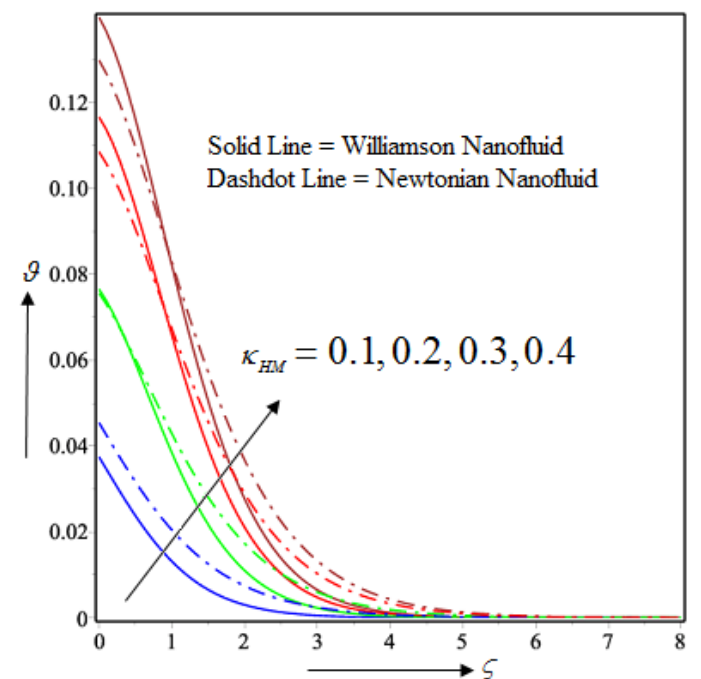
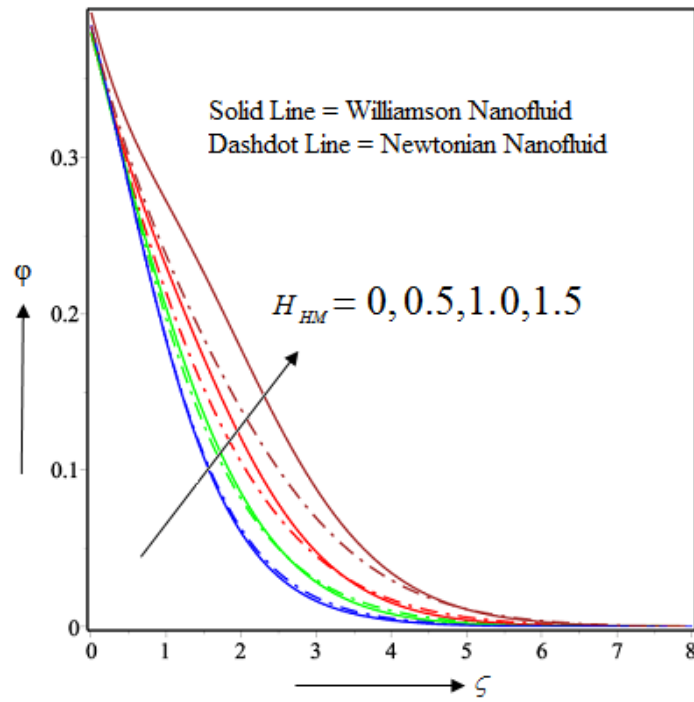


Figure 05:  $\kappa_{HM}$  on the temperature of the flow

profile between two fluids is very much distinct. The influences of  $C_{HT}$  and  $\kappa_{HM}$  are showing similar trend on the temperature of the flow (see Figure 4-5).

**Nanoparticle density profile of the flow:**

In case of nanoparticle concentration is next subject of concern. The  $H_{HM}$  elevates the nanoparticle density of the flow (see Figure 6). But with no homogeneous chemical reaction the densities



1429

Figure 06:  $H_{HM}$  on the concentration of the flow

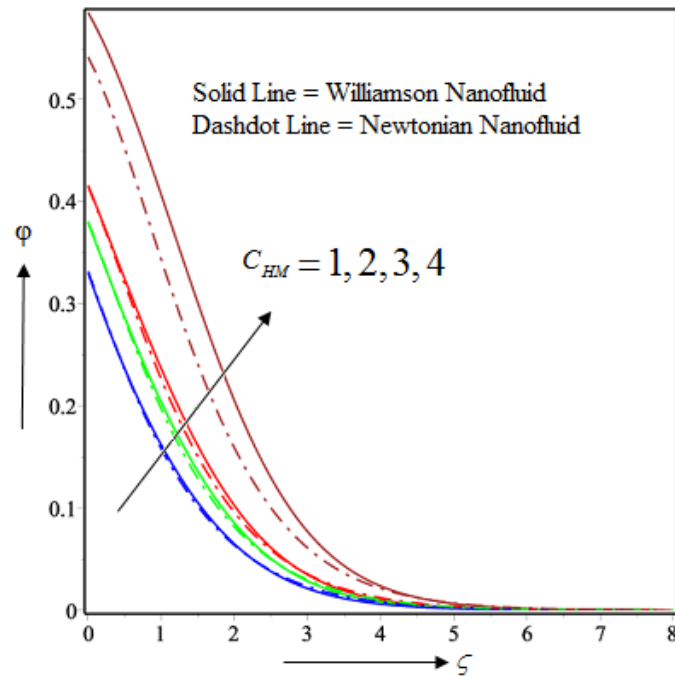
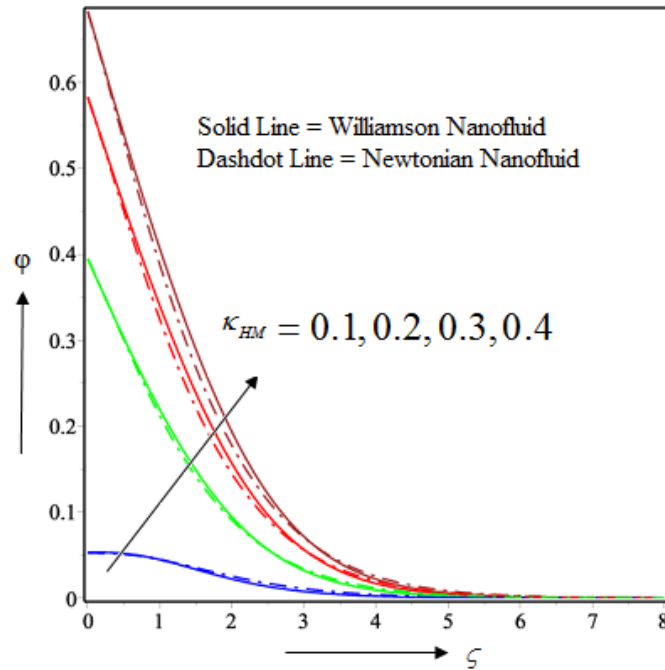


Figure 07:  $C_{HM}$  on the concentration of the flow



1430

Figure 08:  $k_{HM}$  on the concentration of the flow

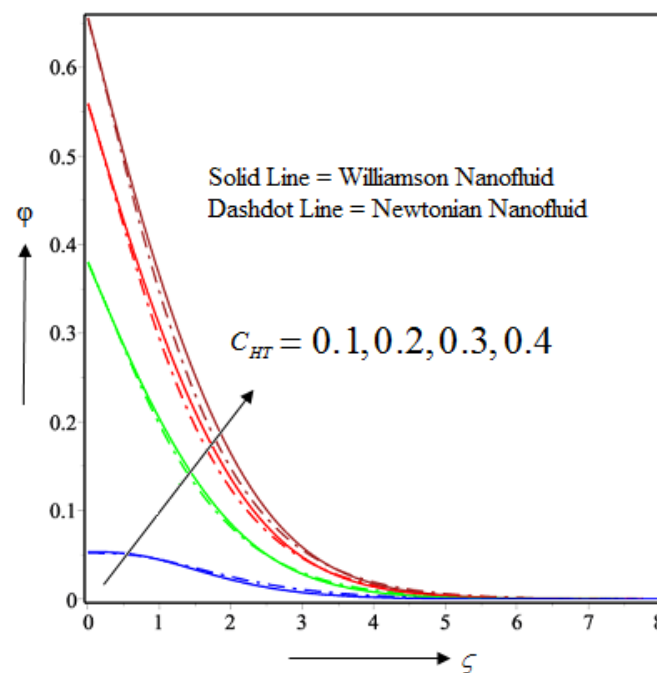


Figure 09:  $C_{HT}$  on the concentration of the flow

of two fluids are almost the same but when more and more chemical reaction takes place the density in the Williamson fluid intensifies rapidly. If the rate of homogeneous chemical reaction rises the nanoparticle volume fraction also increases but in case of Williamson fluid it rises more effectively

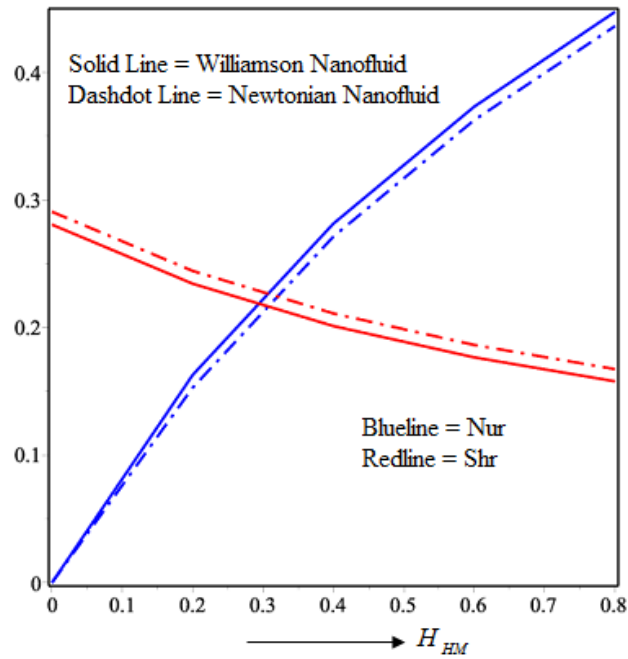


Figure 10:  $H_{HM}$  on the Physical quantities of the flow

1431

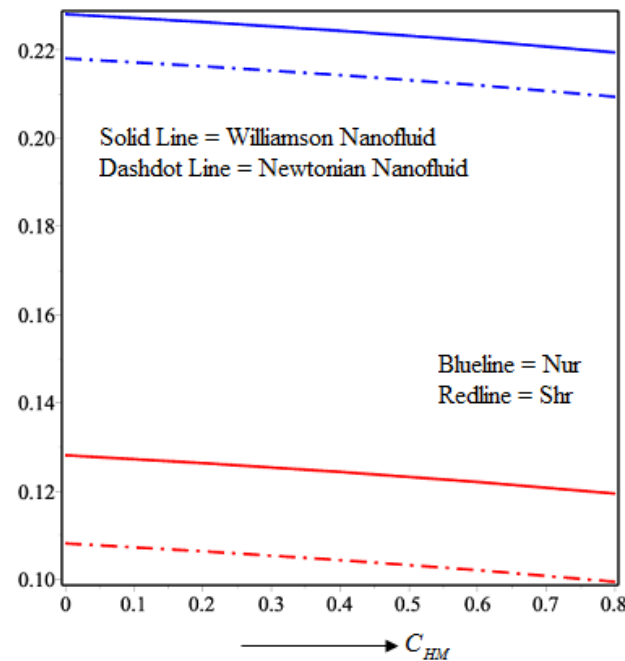
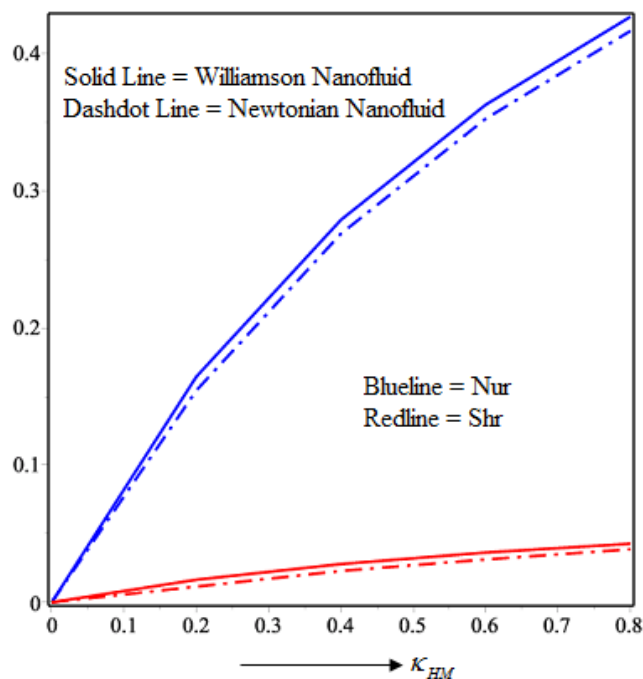


Figure 11:  $C_{HM}$  on the Physical quantities of the flow

(Figure 7). Here  $\kappa_{HM}$  represents the thermal conductivity of the needle surface due to homogeneous chemical reaction. So  $\kappa_{HM}$  increases the heat intake capacity of the fluid and hence it elevates nanoparticle density of the flow more effectively (Figure 8). Similarly, the higher rate of heterogeneous chemical reaction (Figure 9) intensifies the nanoparticle volume fraction of the flow.



1432

Figure 12:  $K_{HM}$  on the Physical quantities of the flow

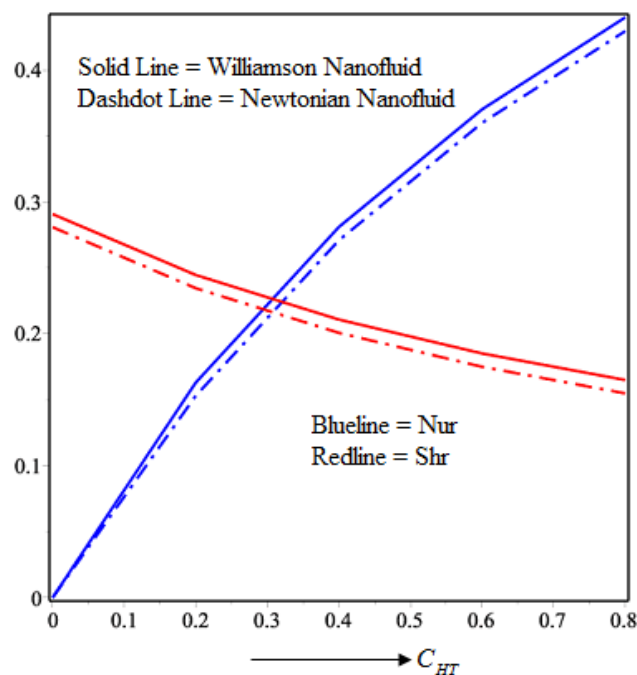


Figure 13:  $C_{HT}$  on the Physical quantities of the flow

**Profile of the physical quantities of the flow:**

The physical measures are meant to measure the performance of the fluid in thermal energy and nanoparticle mass flow. ‘Nur’ represents the heat transfer rate and ‘Shr’ depicts the mass transfer rate. In Figure 10, higher  $H_{HM}$  elevates heat transfer rate while diminishes mass transfer rate. Initially with no

$H_{HM}$  heat transfer for both Newtonian and Williamson fluid are the same and the difference between them elevated with  $H_{HM}$ . But the difference in mass transfer rate is not affected by  $H_{HM}$ . The rate of homogeneous chemical reaction (Figure 11) diminishes both ‘Nur’ and ‘Shr’. In figure 12, ‘Nur’ and ‘Shr’ is



elevated with higher  $\kappa_{HM}$ . But 'Shr' seems lessens with higher  $C_{HT}$  (Figure13).

#### Closing Remarks:

Our results give us more idea about the Williamson Nimonic 80a-Kerosene Nanofluid flowing over thin needle by comparing results of Newtonian Nimonic 80a-Kerosene Nanofluid in the same conditions. After all the analysis we've come to the following concluding remarks.

- A. Temperature of the flow intensifies with homogeneous reaction heat parameter, rate of both reaction and thermal conductivity due to homogeneous reaction.
- B. In all the cases, initially the temperature of the flow is more in case of Williamson fluid but after some distance from the needle it surpasses the temperature of Williamson fluid.
- C. Nanoparticle density also increases with all the parameters of interests. Density is more with the flow of Williamson fluid than Newtonian fluid.
- D. Heat transfer ability of the flow increases with higher  $\kappa_{HM}, C_{HT}, H_{HM}$  and decreases with  $C_{HM}$ .
- E. Mass transfer ability of the flow lessens with  $C_{HM}, C_{HT}, H_{HM}$  and elevates with  $\kappa_{HM}$ .

#### REFERENCES:

[1] Lee LL. Boundary layer over a thin needle. The physics of fluids. 1967 Apr;10(4):820-2.  
[2] Chen JL, Smith TN. Forced convection heat transfer from nonisothermal thin needles. 1978 :358-362.  
[3] Ishak A, Nazar R, Pop I. Boundary layer flow over a continuously moving thin needle in a parallel free stream. Chinese Physics Letters. 2007 Oct;24(10):2895.  
[4] Ahmad S, Arifin NM, Nazar R, Pop I. Mixed convection boundary layer flow along vertical thin needles: Assisting and opposing flows. International communications in heat and mass transfer. 2008 Feb 1;35(2):157-62.

[5] Trimbilas R, Grosan T, Pop I. Mixed convection boundary layer flow along vertical thin needles in nanofluids. International Journal of Numerical Methods for Heat & Fluid Flow. 2014 Apr 1. 24(3), 579-594.

[6] Sulochana C, Ashwinkumar GP, Sandeep N. Joule heating effect on a continuously moving thin needle in MHD Sakiadis flow with thermophoresis and Brownian moment. The European Physical Journal Plus. 2017 Sep 1;132(9):387.

[7] Krishna PM, Sharma RP, Sandeep N. Boundary layer analysis of persistent moving horizontal needle in Blasius and Sakiadis magnetohydrodynamic radiative nanofluid flows. Nuclear Engineering and Technology. 2017 Dec 1;49(8):1654-9.

[8] Sulochana C, Ashwinkumar GP, Sandeep N. Boundary layer analysis of persistent moving horizontal needle in magnetohydrodynamic ferrofluid: A numerical study. Alexandria engineering journal. 2018 Dec 1;57(4):2559-66.

[9] Ahmad R, Mustafa M, Hina S. Buongiorno's model for fluid flow around a moving thin needle in a flowing nanofluid: A numerical study. Chinese journal of physics. 2017 Aug 1;55(4):1264-74.

[10] Salleh SN, Bachok N, Arifin NM, Ali FM, Pop I. Stability analysis of mixed convection flow towards a moving thin needle in nanofluid. Applied Sciences. 2018 Jun;8(6):842.

[11] Choi SU, Eastman JA. Enhancing thermal conductivity of fluids with nanoparticles. Argonne National Lab., IL (United States); 1995 Oct 1.

[12] Buongiorno, J. Convective transport in nanofluids. 2006: 240-250.

[13] Bhaskar Reddy N., Poornima T. and Sreenivasulu P., Radiative heat transfer effect on MHD slip flow of dissipating nanofluid past an exponential stretching porous sheet. International Journal of Pure and Applied Mathematics, 109, 9, 2016, pp.134 – 142. <http://www.ijpam.eu>

[14] Sreenivasulu P., Poornima T. and Bhaskar Reddy N., Thermal radiation effects on MHD boundary layer slip flow past a permeable exponential stretching sheet in the presence of joule heating and viscous dissipation.

Journal of Applied Fluid Mechanics, 9,1, 2016, pp.267-278.

[15] Tamoor M., MHD convective boundary layer slip flow and heat transfer over nonlinearly stretching cylinder embedded in a thermally stratified medium, Results in Physics, 7, 2017, pp.4247-4252. <https://doi.org/10.1016/j.rinp.2017.07.064>

[16] Parida S.K., Panda S. and Rout B. R., MHD boundary layer slip flow and radiative nonlinear heat transfer over a flat plate with variable fluid properties and thermophoresis, Alexandria Engineering Journal, 54, 4, 2015, pp.941-953. <https://doi.org/10.1016/j.aej.2015.08.007>.

[17] Nayak M.K., Shaw S., Chamkha A.J., Impact of variable magnetic field and convective boundary condition on a stretched 3D radiative flow of Cu-H<sub>2</sub>O nanofluid, AMSE JOURNALS-AMSE IETA publication-2017-Series: Modelling B; 86, 3, 2018, pp.658-678. ed Jan. [https://doi.org/10.18280/mmc\\_b.860305](https://doi.org/10.18280/mmc_b.860305)

[18] Nayak M.K., Akbar N. S., Tripathi D. and Pandey V.S., Three dimensional MHD flow of nanofluid over an exponential porous stretching sheet with convective boundary conditions, Thermal Science and Engineering Progress, 3, 2017, pp.133- 140. DOI: 10.1016/j.tsep.2017.07.006

[19] Das S., Sensharma A., Jana R. N., Sharma R. P., Slip flow of nanofluid past a vertical plate with ramped wall temperature considering thermal radiation, Journal of Nanofluids, 6, 6, 2017, pp.1054-1064. DOI: <https://doi.org/10.1166/jon.2017.1392>

[20] Abbas Z., Naveed M. and Sajid M., Hydromagnetic slip flow of nanofluid over a curved stretching surface with heat generation and thermal radiation, Journal of Molecular Liquids, 215, 2016, pp.756-762.

[21] Tausif S.K.Md., Kalidas D. and Prabir Kumar K., Effect of magnetic field on slip flow of nanofluid induced by a non-linear permeable stretching surface, Applied Thermal Engineering, 104, 5, 2016, pp.758-766. <https://doi.org/10.1016/j.applthermaleng.2016.05.129>

[22] Farooq M., Ijaz Khan M., Waqas M., Hayat T., Alsaedi A. and Imran Khan A., MHD

stagnation point flow of viscoelastic nanofluid with non-linear radiation effects, Journal of Molecular Liquids, 221, 2016, pp.1097–1103. <http://dx.doi.org/10.1016/j.molliq.2016.06.077>.

[23] Bhatti MM, Rashidi MM. Effects of thermo-diffusion and thermal radiation on Williamson nanofluid over a porous shrinking/stretching sheet. Journal of Molecular Liquids. 2016 Sep 1;221:567-73.

[24] Naseer M, Malik MY, Nadeem S, Rehman A. The boundary layer flow of hyperbolic tangent fluid over a vertical exponentially stretching cylinder. Alexandria engineering journal. 2014 Sep 1;53(3):747-50.

[25] Hamid A, Khan M. Numerical simulation for heat transfer performance in unsteady flow of Williamson fluid driven by a wedge-geometry. Results in Physics. 2018 Jun 1;9:479-85.

[26] Hayat T, Ahmad S, Khan MI, Alsaedi A. Exploring magnetic dipole contribution on radiative flow of ferromagnetic Williamson fluid. Results in physics. 2018 Mar 1;8:545-51.

[27] Lund LA, Omar Z, Khan I. Analysis of dual solution for MHD flow of Williamson fluid with slippage. Heliyon. 2019 Mar 1;5(3):e01345.

[28] Raju CS, Sandeep N, Ali ME, Nuhait AO. Heat and mass transfer in 3-D MHD Williamson-Casson fluids flow over a stretching surface with non-uniform heat source/sink. Thermal Science. 2019; 23(1):281-93.

1434